10.1098/rsta.2001.0828

THE ROYAL SOCIETY

Modelling cardiac mechanical properties in three dimensions

By Kevin D. Costa[1], Jeffrey W. Holmes[1] and Andrew D. McCulloch[2]

[1]*Department of Biomedical Engineering, Columbia University MC 8904, 530 W. 120th Street, New York, NY 10027, USA*
[2]*Department of Bioengineering, Whitaker Institute of Biomedical Engineering, University of California San Diego, La Jolla, CA 92093-0412, USA*

The central problem in modelling the multi-dimensional mechanics of the heart is in identifying functional forms and parameters of the constitutive equations, which describe the material properties of the resting and active, normal and diseased myocardium. The constitutive properties of myocardium are three dimensional, anisotropic, nonlinear and time dependent. Formulating useful constitutive laws requires a combination of multi-axial tissue testing *in vitro*, microstructural modelling based on quantitative morphology, statistical parameter estimation, and validation with measurements from intact hearts. Recent models capture some important properties of healthy and diseased myocardium including: the nonlinear interactions between the responses to different loading patterns; the influence of the laminar myofibre sheet architecture; the effects of transverse stresses developed by the myocytes; and the relationship between collagen fibre architecture and mechanical properties in healing scar tissue after myocardial infarction.

Keywords: myocardium; constitutive model; biaxial testing; mechanics

1. Introduction

The mechanics of the heart are inherently multi-dimensional. The means by which the forces generated by linear arrays of sarcomeres are converted to chamber pressures depends on the three-dimensional geometry and myofibre architecture of the ventricular myocardium. Three-dimensional imaging has shown that regional wall motions and myocardial strains do not lend themselves to two-dimensional simplification. All the components of the three-dimensional strain tensor can be significant in magnitude.

While myocardial strains can be measured, regional stresses (the forces of interaction between adjacent tissue elements) cannot. Therefore, mathematical models are needed to interpret experimental and clinical observations on regional myocardial deformations, to identify material properties underlying the behaviour of the intact heart, and to integrate mechanical properties measured in isolated filaments, cells and tissues into models of the intact heart.

Using continuum mechanics as a foundation, the problem of modelling cardiac mechanics has the following components: ventricular geometry and structure; pressure and displacement boundary conditions; the partial differential equations gov-

erning the conservation of mass, momentum and energy; and most importantly, the constitutive laws that describe the mechanical responses of resting and contracting cardiac muscle and their regional and temporal variations. Because the problem is nonlinear, dynamic and three-dimensional, numerical methods are essential for accurate quantitative analysis. Many aspects of the problem are covered elsewhere: LeGrice *et al*. (2001) focuses on quantitative and parametric descriptions of ventricular anatomy and structure. The boundary conditions are simply the haemodynamic pressures on the cardiac chambers and the constraints of the pericardium and surrounding tissues. The most suitable numerical method for modelling myocardial mechanics is the finite-element method, which is a well-established technique (Guccione & McCulloch 1991).

In this article, we review a critical challenge in myocardial mechanics: developing accurate constitutive models that describe how the structure and biophysics of the normal and diseased myocardium give rise to the mechanical responses of the intact tissue. This in turn requires an understanding of myocardial structure and material testing, and regional mechanical behaviour of the heart walls observed *in vivo*. While much of the work in this field builds on uniaxial and two-dimensional studies, we focus primarily on three-dimensional measurements and models.

2. Modelling passive ventricular myocardium

The structure and organization of the muscle fibres and extracellular matrix give rise to the macroscopic material symmetry and mechanical properties of the resting tissue, which in turn determine its mechanical function. Many investigators have attempted to deduce myocardial resting material properties from the end-diastolic pressure–volume relation and information on regional wall geometry. While this approach can yield some information about the overall stiffness of the chamber, material properties identified from these global measurements are not useful for studying the regional mechanics of the myocardium or for relating material behaviour to the three-dimensional structure of the wall.

One of the simplest and most widely used material testing protocols is the uniaxial tension test. Laser diffraction also makes it possible to measure sarcomere length under these conditions in small multicellular preparations like right ventricular trabeculae (ter Keurs 1995). However, such uniaxial stress–strain data are inherently insufficient to characterize the three-dimensional constitutive behaviour of the myocardium. Triaxial tissue testing is ideal, but it remains challenging in practice due to technical limitations (Halperin *et al.* 1987).

(*a*) *Biaxial testing of excised myocardium*

Because passive, unperfused ventricular myocardium is nearly incompressible, biaxial tissue testing is a valuable method for characterizing its three-dimensional material properties. Biaxial tests most commonly involve orthogonal loading of thin rectangular tissue slices cut parallel to the epicardial surface so that the muscle fibres lie within the plane of the tissue sample and the predominant fibre direction is aligned with one edge of the sample. In the first biaxial tests of excised passive myocardium, Demer & Yin (1983) observed that the nonlinear, viscoelastic properties of resting myocardium are anisotropic, and approximately pseudo-elastic. Therefore, myocardium is frequently modelled as a finite hyperelastic material, where the

components of the second Piola–Kirchhoff stress, P_{ij}, are related to the Lagrangian Green's strain E_{ij}, through the pseudo-strain energy, W,

$$P_{ij} = \frac{1}{2}\left(\frac{\partial W}{\partial E_{ij}} + \frac{\partial W}{\partial E_{ij}}\right) - pC_{ij}^{-1}, \tag{2.1}$$

where C_{ij} is the right Cauchy–Green deformation tensor ($\boldsymbol{C} = 2\boldsymbol{E} + \boldsymbol{I}$), I is the identity tensor, and p is a hydrostatic pressure Lagrange multiplier, which does not contribute to the deformation of an incompressible material and must be computed from the governing equations and boundary conditions. The functional form of W is often estimated by curve-fitting experimental measurements (Gupta *et al.* 1994), which complicates the interpretation of parameters and generalization to other conditions.

Using a more rational approach, Humphrey *et al.* (1990*a*) designed specific biaxial tests to determine the functional form of W directly from the data, resulting in the following polynomial function:

$$W = c_1(\alpha - 1)^2 + c_2(\alpha - 1)^3 + c_3(I_1 - 3) + c_4(I_1 - 3)(\alpha - 1) + c_5(I_1 - 3)^2. \tag{2.2}$$

The material symmetry of this formulation is a subclass of transverse isotropy where I_1 is the first principal strain invariant and the transversely isotropic invariant α is the extension ratio in the fibre direction. Both can be expressed in terms of the strain components,

$$I_1 = 2\,\mathrm{tr}\,\boldsymbol{E} + 3; \qquad \alpha = \sqrt{2E_{ff} + 1}, \tag{2.3}$$

where E_{ff} is the strain along the muscle fibre direction. An important observation in that study was the discovery of an interaction between the isotropic and anisotropic terms ($c_4 \neq 0$).

The choice of constitutive model influences the conclusions of biaxial experiments. Studies using ad hoc constitutive formulations found that ventricular myocardium is 1.5 to 3 times stiffer in the fibre direction than the cross-fibre direction (Humphrey *et al.* 1990*b*; Sacks & Chuong 1993; Yin *et al.* 1987). With equation (2.2), Novak and coworkers (Novak *et al.* 1994) obtained material parameters from biaxial stress–strain measurements in the subepicardium, midwall, and subendocardium of the passive canine left ventricular free wall and septum. Although fibre stiffness was consistently greater than cross-fibre stiffness, there were no significant regional variations in the degree of anisotropy. However, the total strain energy of the deformation was greater for the inner and outer wall specimens than for the midwall, suggesting that ventricular myocardium is transmurally inhomogeneous.

From such studies, it is difficult to delineate the mechanical role of different myocardial tissue constituents because their structural interactions are also important. However, it is evident that the composite myocardium is stiffer at rest than the isolated myocyte, and that the collagen extracellular matrix contributes anywhere from 20 to 80% of passive stiffness in the intact muscle (Granzier & Irving 1995). The collagenous epicardium and parietal pericardium are distinctly different in material properties from myocardium, being more compliant and isotropic at low biaxial strains and much stiffer and more anisotropic at higher strains (Humphrey *et al.* 1990*c*). Biaxial tests also indicated that the epicardium may significantly influence the mechanics of the underlying subepicardial muscle (Kang & Yin 1996).

Table 1. *Material parameters of an exponential transversely isotropic strain energy function in equation (2.4)*

	C (kPa)	b_1	b_2	b_3
canine epicardium[a]	0.88	18.5	3.58	1.63
canine midwall[b]	1.2	26.7	2.0	14.7
rat midwall[b]	1.1	9.2	2.0	3.7

[a]Guccione *et al.* (1991); [b]Omens *et al.* (1993).

(*b*) *Experiments in isolated arrested hearts*

One difficulty with any constitutive model based only on biaxial tissue tests is uncertainty as to how the biaxial properties of isolated tissue slices are related to the properties of the intact ventricular wall. Whereas shear deformations are an important component of three-dimensional mechanics in the intact heart (Omens *et al.* 1991), the standard biaxial protocol does not test the material under shear deformations, and a new biaxial protocol that includes in-plane shear (Sacks 1999) has not yet been applied to myocardial tissue. Furthermore, variation of the fibre direction through the thickness of the tissue sample makes it difficult to extract an accurate fibre and cross-fibre stiffness (Novak *et al.* 1994). It is also difficult to assess the extent to which excising a thin sample alters the material properties of the tissue.

Guccione and co-workers (Guccione *et al.* 1991) used a different approach to identifying constitutive parameters. Considering the fibrous structure of the myocardium, they selected a transversely isotropic, exponential strain energy function,

$$W = \tfrac{1}{2}C(\exp(Q) - 1), \tag{2.4}$$

where

$$Q = b_1 E_{ff}^2 + b_2(E_{cc}^2 + E_{rr}^2 + 2E_{cr}E_{rc}) + 2b_3(E_{fc}E_{cf} + E_{fr}E_{rf}),$$

in terms of strain components E_{ij} referred to a system of local fibre, cross-fibre and radial coordinates (f, c, r). By analysing the inflation, stretch, and twist of a thick-walled cylinder, they identified material parameters (table 1) using a semi-inverse method to match epicardial strains measured in isolated arrested canine hearts. Accounting for the variation in fibre orientation through the wall, they estimated that the myocardium was two to three times stiffer in the fibre direction than the cross-fibre direction. This approach has the advantage that it used measurements from the intact ventricle, but it neglects regional inhomogeneities.

Other studies (Emery & Omens 1997; Emery *et al.* 1997; Omens *et al.* 1993) used similar inverse methods to identify material parameters for rat myocardium. Omens and co-workers (Omens *et al.* 1993) found less anisotropy in the rat than in the dog (table 1). Note that these estimates based on midwall strains are different than the earlier ones based on epicardial data. Emery *et al.* (1997) found substantial and isotropic decreases in fibre and cross-fibre stiffnesses during acute volume overloading in the isolated rat heart, whereas diastolic muscle stiffness increased 10-fold in the hypertrophied rat heart during six weeks of chronic volume overload (Emery & Omens 1997). While the acute changes may reflect failure of interlaminar collagen ties (Emery *et al.* 1998), the mechanism of the chronic stiffening is unknown but may be related to increased collagen crosslinking (Iimoto *et al.* 1988).

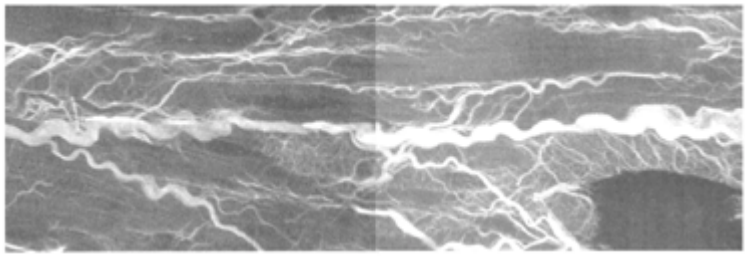

Figure 1. Composite view of perimysial collagen fibres in rat ventricular myocardium, obtained by confocal microscopy of picrosirius red stained tissue. 60× oil immersion objective. Image volume = 278 × 93 × 12 (depth) μm. The left and right sides of the image are each extended focus views through 25 optical sections 0.5 μm apart. (Courtesy of William Karlon.)

(*c*) *Structural evidence for material orthotropy*

The strain energy functions above are transversely isotropic, having a single preferred axis along the muscle fibre direction. Microstructural evidence of a regular distribution of endomysial collagen struts around myocytes and long coiled perimysial fibres (MacKenna *et al.* 1997) parallel to them (figure 1) has been used to justify the assumption of transverse isotropy. However, as described in the article by LeGrice *et al.* (2001), ventricular myofibres are organized into branching laminae, suggesting that myocardium may be locally orthotropic having distinct cross-fibre stiffnesses within and across the sheet planes. Regional variations in sheet orientation and branching are also significant (LeGrice *et al.* 1995*a*).

To extend the constitutive model to material orthotropy, we begin by defining a system of locally Cartesian base vectors defining a fibre–sheet–normal coordinate system $\{X_\mathrm{f}, X_\mathrm{s}, X_\mathrm{n}\}$ with one axis parallel to the muscle fibres, one parallel to the sheets and perpendicular to the fibres, and the third normal to the sheet plane. Then, Q in equation (2.4) can then be generalized:

$$Q = c_1(E_{\mathrm{ff}}^2) + c_2(E_{\mathrm{ss}}^2) + c_3(E_{\mathrm{nn}}^2) + 2c_4(E_{\mathrm{fs}}E_{\mathrm{sf}}) + 2c_5(E_{\mathrm{fn}}E_{\mathrm{nf}}) + 2c_6(E_{\mathrm{sn}}E_{\mathrm{ns}}). \quad (2.5)$$

c_1, c_2 and c_3 represent stiffnesses along the fibre, sheet and sheet-normal axes, respectively. c_2/c_3 governs anisotropy in the plane normal to the local fibre axis, with unity indicating transverse isotropy. c_4 represents the shear modulus in the sheet plane, and c_5 and c_6 represent shear stiffness between adjacent sheets.

Recently, Nash & Hunter (2001) proposed a 'pole-zero' formulation of the pseudo-strain energy function with 18 material constants describing uniaxial and shear behaviour with respect to the three orthogonal structural axes (i.e. $X_\mathrm{f}, X_\mathrm{s}, X_\mathrm{n}$ above). One common difficulty with structurally based constitutive models is the large number of required model parameters. But these authors recognized that axial and shear deformations are probably strongly correlated because they involve the same underlying microstructure. Assuming distributions of collagen fibre families, they used a kinematic analysis to reduce the number of independent unknown material parameters based on structural considerations. Although the assumed microstructure was not based on histological measurements, such a microstructural constitutive law is appealing for its direct physical interpretation of material parameters. An earlier (uniaxial) microstructural analysis that was based directly on measured collagen fibre morphology (MacKenna *et al.* 1997) does support the assumption of collagen fibres underlying the pole-zero formulation.

(*d*) *Residual stress*

A fundamental consideration in constitutive modelling is the reference state for stress and strain. In general, the stress-free state in tissues is not necessarily the unloaded state (i.e. in the absence of any external tractions or pressures); ventricular myocardium and other tissues are residually stressed (Omens & Fung 1990). Residual stress is thought to arise from tissue growth and remodelling (Rodriguez *et al.* 1994), and its presence must be accounted for to accurately model the biaxial mechanics of composite myocardium from measurements of its constituent material properties (Kang & Yin 1996).

Residual stress has been shown to influence the transmural distribution of diastolic sarcomere lengths (Rodriguez *et al.* 1993), thereby influencing subsequent systolic fibre tension development. Residual stress has also been observed to reduce endocardial stress concentrations in continuum models (Guccione *et al.* 1991). These analyses assumed that an open cylindrical arc accurately represents the stress-free state of the ventricle. Costa *et al.* (1997) observed a considerably more complex stress-free configuration in the canine left ventricle when measurements of three-dimensional transmural residual strains were found to include substantial longitudinal, torsional and transverse shear components, implicating laminar myocardial sheets as important structures bearing residual stress in the left ventricle. Incorporating such a three-dimensional residual stress state into the myocardial constitutive formulation is a complex problem for which a general theoretical framework has only recently become available (Johnson & Hoger 1995).

(*e*) *New directions*

A common problem with estimating parameters of the strain energy function, whether directly from isolated tissue testing or indirectly from strains measured in the intact heart, is that the functions are nonlinear. More fundamentally, the kinematic response terms, whether principal invariants (equation (2.2)) or strain components (equation (2.4)), usually co-vary under any real loading condition. This is probably the main factor responsible for the very wide variation in parameter estimates between individual mechanical tests that is typically reported. The parameter estimation could be greatly improved if an orthogonal set of response terms could be found. Recently, Criscione *et al.* (2001) achieved precisely that for the case of transverse isotropy. By kinematically separating volume change from fibre extension and shearing distortions, the resulting set of response terms should provide an improved foundation for myocardial constitutive modelling.

Biomechanical testing in genetically altered animal models is a recent development that is permitting the structural basis of tissue mechanics to be probed more specifically. For example, Weis *et al.* (2000) observed significantly lower myocardial fibre stiffness and substantially increased residual strains associated with type I collagen deficiency in the *osteogenesis imperfecta murine* compared with wild-type littermates.

3. Modelling active ventricular myocardium

A long history of experimental and theoretical studies on the mechanics of muscle contraction has provided a foundation for integrated models of myocardial mechan-

ics. The vast majority of experimental studies have been based on one-dimensional measurements of force, length and velocity in isolated muscles or cardiomyocytes. Mathematical models of one-dimensional force generation have also reached a comparatively advanced state, incorporating the biophysics and energetics of thin filament activation (Michailova & Spassov 1997) and crossbridge interactions (Landesberg *et al.* 1995), though the mechanisms of cooperativity between activation and crossbridge interaction remain unclear. By modelling several alternative mechanisms of this cooperativity, Rice *et al.* (1999) concluded that modelling end-to-end interactions between adjacent troponin and tropomyosin molecules best reproduced experimental observations. For more detailed background on experimental and theoretical studies on uniaxial cardiac muscle mechanics, we refer the reader to an excellent review (ter Keurs 1995). But from a continuum modelling perspective, we may summarize by saying that active myofibre stress development in isolated cardiac muscle is a function not only of sarcomere length (strain), but also of the velocity of shortening (rate of strain), and the time history of length (strain history).

(*a*) *Modelling active fibre stress in a continuum*

When the myocardium is assumed to be transversely isotropic, active fibre stress may be incorporated into the constitutive formulation by summing the contributions of the fibre-directed active stress and passive stress due to tissue deformation. Guccione and co-workers (Guccione *et al.* 1993) used a cylindrical model to compare three alternative models of active tension development: a length-history dependent 'deactivation' model that could predict deactivation in response to rapid length perturbations; a 'Hill' model based on the force–velocity relation, but without transient deactivation; and a 'time-varying elastance' model in which tension depended only on sarcomere length and time. Despite significant differences in the time courses of stress and sarcomere length, at end-systole the 'Hill' and 'time-varying elastance' models were nearly identical. Larger end-systolic fibre stresses were observed with the deactivation model, but the wall stress distribution was minimally affected. Thus, due to its simple formulation, the time-varying elastance model remains preferred in most continuum analyses of systolic myocardial mechanics, but future continuum models must incorporate more dynamic detail so that they can reflect the biophysics of crossbridge interactions more accurately.

(*b*) *Cross-fibre force generation*

While cardiac muscle contraction has been studied extensively in one dimension, experimental information on the multi-dimensional contractile properties of myocardium is scarce. Lin & Yin (1998) made an important contribution, when they succeeded in performing biaxial tests on sheets of rabbit ventricular myocardium tonically activated by barium perfusion or rapid pacing in the presence of ryanodine. They observed unexpectedly high systolic force development along the cross-fibre axis (exceeding 40% of the fibre stress during equibiaxial loading). The mechanisms of this substantial transverse active stress remain unknown, but likely candidates include the crossbridge lattice geometry (Schoenberg 1980*a*; Zahalak 1996) and the 12–15° dispersion of myofibre angles about the mean (Karlon *et al.* 1998). Theoretical analyses based on crossbridge lattice geometry also suggest that large transverse deformations can alter stress development along the myofilament axis (Schoenberg

1980*b*). Extending the analysis to a model of the contracting left ventricle, Zahalak *et al.* (1999) observed that non-axial deformations could reduce active fibre stress as much as 35%, depending on the location in the wall. Developing a comprehensive theory that integrates crossbridge biophysics and tissue microarchitecture and reconciles detailed one-dimensional data with emerging multiaxial measurements remains a significant task in modelling and understanding myocardial mechanics.

(*c*) *Experimental evidence for orthotropy*

Measurements of three-dimensional myocardial deformation from end-diastole to end-systole in experimental animals and man reveal a complex combination of radial wall thickening, circumferential and longitudinal shortening, torsion of the apex relative to the base, and substantial shear strains in long- and short-axis planes of the ventricle (LeGrice *et al.* 1995*b*; Waldman *et al.* 1988). The three-dimensional myofibre architecture of the myocardium has also been extensively studied, but it remains unclear how simple axial shortening of individual myocytes is transformed into the complex deformation required for efficient ejection of blood from the heart.

To provide insight into the structural basis of systolic strains, Waldman *et al.* (1988) constructed a set of coordinate axes defined by the local muscle fibre orientation. In canine mid-ventricular free wall tissue, they found end-systolic strain along the muscle fibre axis was relatively uniform transmurally, whereas radial wall-thickening strain had a substantial transmural gradient and was greatest in the subendocardium. Surprisingly, cross-fibre shortening in the epicardial-tangent plane far exceeded fibre shortening in the subendocardium, and has been strongly correlated with regional systolic wall thickening (Rademakers *et al.* 1994). If we make the simple assumption that the myocyte behaves like an incompressible cylinder, it is clear that the 4% increase in cell diameter associated with the measured 7% fibre shortening cannot account for the measured 30% local wall thickening strain or the 17% cross-fibre shortening measured in these studies. Therefore, myocytes must undergo some shape change or rearrangement to yield substantial subendocardial wall thickening during systole.

Feneis (1943) originally speculated that the laminar organization of the myocardium may permit rearrangement of muscle fibre bundles by sliding along cleavage planes. Supporting this idea, Spotnitz *et al.* (1974) observed that a 15° change in cleavage plane orientation toward the radial direction could increase the number of cells across the wall and account for wall thickening during systolic contraction. LeGrice and co-workers (LeGrice *et al.* 1995*b*) tested this mechanism by comparing three-dimensional systolic strains and sheet orientations in the canine left ventricle. Despite large regional differences in strain and tissue structure, they found a consistent systolic reorientation of subendocardial laminae by about 12°, which accounted for over 50% of measured local systolic wall thickening. Later, Costa *et al.* (1999) measured systolic strains with respect to local fibre-sheet axes at several sites in the canine ventricular free wall, and analysed their relationship to wall thickening. This revealed a regionally consistent trend that lateral extension of laminar cell bundles is responsible for about 60% of wall thickening, while interlaminar shearing largely accounts for the rest. Hence, the sheet arrangement of myofibres may provide a fundamental mechanism for converting relatively small and uniform fibre shortening into large and non-uniform wall thickening during systole.

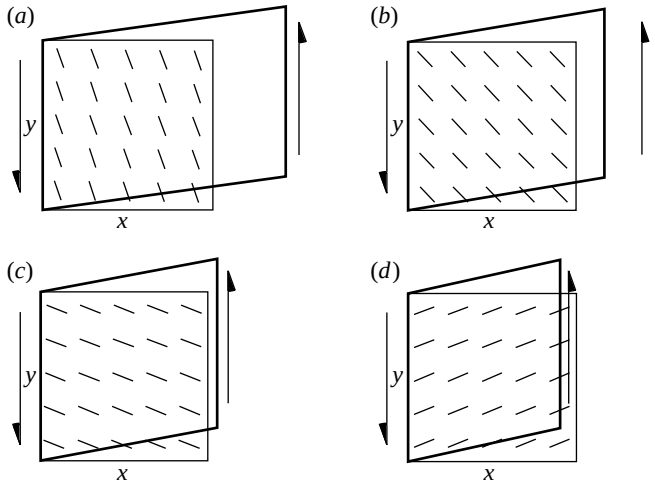

Figure 2. Finite-element models of transverse shear in an orthotropic, incompressible unit cube. x- and y-axes represent local radial and cross-fibre directions, respectively. Short lines are undeformed sheet orientation (angle β), with muscle fibres aligned uniformly along the z-axis perpendicular to the shear plane. The endocardium ($x = 0$) was fixed, a positive displacement was applied to the epicardial face ($x = 1$) producing a 10% transverse shear, and the equilibrium configuration of the cube was obtained with the radial (x) displacement unconstrained. Dark lines indicate the deformed equilibrium configuration. Panels show (*a*) $\beta = -70°$, (*b*) $\beta = -45°$, (*c*) $\beta = -20°$, (*d*) $\beta = 20°$.

To test whether orthotropic material properties suggested by the laminar tissue architecture are important for the experimentally observed relationship between laminar sheet orientation, transverse shearing and wall thickening during systole, we formulated a simple finite-element model of a cube of myocardium (figure 2). The model assumed a homogeneous sheet orientation and an orthotropic strain energy function defined by equation (2.5), using a value of c_2 100-fold greater than the other coefficients to model stiff myocardial laminae. Applied transverse shear did influence wall thickness: the amount of wall thickening decreased as the sheet angle approached zero, and wall thinning occurred when the sheet angle changed sign without a corresponding change in the shear. In contrast, for a transversely isotropic material (not shown) shear always led to wall thinning. Thus, for reorientation of cleavage planes to provide a mechanism for systolic wall thickening, it will be necessary to replace the assumption of transverse isotropy with a more realistic material description that reflects the underlying layered architecture of myocardial tissue.

(*d*) *Validating constitutive laws using three-dimensional models*

The final step in modelling the constitutive behaviour of myocardium is model validation. In addition to fitting the data from which the material parameters were derived, a useful constitutive model should be able to predict tissue behaviour for other loading conditions as well. Material properties obtained from specific biaxial tests have been used to predict the results of different loading protocols (Humphrey *et al.* 1990*b*; Kang & Yin 1996). But ultimately we wish to obtain a constitutive model that is appropriate for the three-dimensional loading conditions of the beating heart. In contrast to the various methods for measuring regional myocardial

strains, reliable measurement of local wall stress in the intact heart has remained largely unsuccessful. Therefore, one validation approach is to compare estimated strains from computational models subjected to physiological loading pressures with corresponding experimental strains. The finite-element method is particularly well suited for this modelling task due to its ability to incorporate the three-dimensional geometry, fibrous tissue architecture, pressure boundary conditions, and nonlinear material properties of the tissue (Guccione & McCulloch 1991). If it can be shown that a model accurately describes experimental three-dimensional strains, then this provides confidence in the estimated stresses, which are important for understanding myocardial growth and remodelling in physiological and pathophysiological conditions. Alternatively, identifying the source of discrepancies between estimated and measured strains by testing the model assumptions can provide useful insight into the main determinants of regional cardiac mechanics.

Guccione *et al.* (1995) constructed an axisymmetric model of the passive canine left ventricle incorporating a realistic longitudinal geometric profile and fibre distribution and transversely isotropic material properties (equation (2.4)). The model agreed well with transmural strain distributions measured in isolated dog hearts (Omens *et al.* 1991), except for an insufficient gradient in longitudinal strain and an over-estimation of the magnitude of circumferential–radial shear strain (figure 3). We repeated this analysis using the constitutive relation in equation (2.2), with material parameters scaled to give a similar passive pressure–volume relation, and the predicted strains did not differ substantially from those in figure 3. More recently, Vetter & McCulloch (2000) described a model of passive filling in the rabbit heart based on a very detailed anatomical reconstruction of right and left ventricular geometry and fibre architecture. The model reproduced measured epicardial strains well.

Finite-element models of systolic ventricular function have also been developed. Bovendeerd *et al.* (1994) used an axisymmetric model, with a transversely isotropic constitutive law and a modified Hill model of myofibre contraction to demonstrate the significant influence of the small out-of-plane component of fibre orientation (imbrication angle) on ventricular mechanics during systole. Circumferential–radial transverse shear was the component most sensitive to imbrication angle and torsional shears agreed better with observation when the out-of-pane component of fibre angle was included. Later Rijcken *et al.* (1999) treated fibre helical and imbrication angles as unknowns in a mechanical optimization. Searching for muscle fibre angle distributions that minimized regional variations in sarcomere shortening during ejection, they predicted muscle fibre architectures that were remarkably similar to those measured by histology and diffusion tensor magnetic resonance imaging. An axisymmetric porous medium finite-element model of the beating left ventricle (Huyghe *et al.* 1992) allowed relative motion of solid and fluid phases in the myocardium. Model results were similar to measurements of systolic principal strains (Waldman *et al.* 1988), but could not accurately reproduce observed transverse shears.

Guccione and co-workers (Guccione *et al.* 1995) included active contraction in the axisymmetric canine left ventricular model described earlier. Compared with measured systolic strains (Waldman *et al.* 1988), there was good agreement for the three in-plane strain components but again transverse shear strains were not accurately estimated. We wondered whether material orthotropy might explain the discrepancy

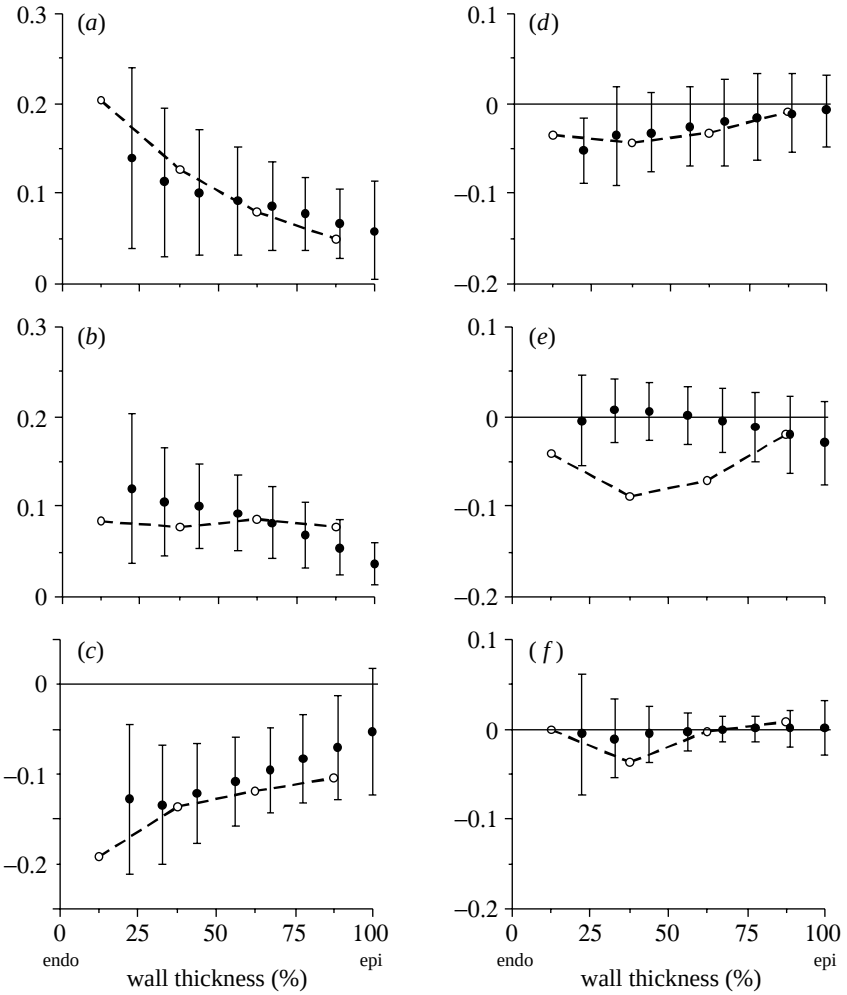

Figure 3. Transmural distributions of midwall strain during filling to 7.5 mm Hg of the canine left ventricle. Open symbols are from the finite-element model of Guccione *et al.* (1995) and closed symbols are mean measurements from Omens *et al.* (1991) in isolated heart. Panels show (*a*) E_{cc}, (*b*) E_{ll}, (*c*) E_{rr}, (*d*) E_{cl}, (*e*) E_{cr}, (*f*) E_{lr}, referred to local circumferential, longitudinal and radial (*c, l, r*) coordinates.

between transverse shear strains computed with these transversely isotropic models and those measured experimentally. Finite-element model analysis (Usyk *et al.* 2001) showed that orthotropic resting material properties with decreased interlaminar tensile and shearing stiffnesses did improve agreement with diastolic strains, but had disappointingly little effect on the much larger discrepancies seen in the systolic strains. However, a very substantial effect was obtained by incorporating transverse active stress development as observed by Lin & Yin (1998). The preliminary model analysis suggests this mechanism, rather than the sheet structure, may be primarily responsible for the discrepancies in earlier models of systolic ventricular mechanics.

4. Myocardial infarction: modelling healing scar

Following myocardial infarction, ischaemic segment shortening rapidly converts to systolic lengthening. Over the subsequent days and weeks, the damaged area undergoes necrosis, then fibrosis, with collagen content increasing steadily for six weeks or more. Modelling efforts have primarily focused on the impact of a non-contracting segment on overall ventricular function, with the size of the damaged region being the critical variable (Janz & Waldron 1977). Less attention has been given to the material properties of infarcted and healing myocardium. Acutely ischaemic myocardium has been modelled as fully passive (Bogen *et al.* 1980) or having reduced myofilament calcium sensitivity (Mazhari *et al.* 2000), while necrotic myocardium has been modelled as passive tissue with increased stiffness (Bogen *et al.* 1980) or as a fluid surrounded by a muscular capsule (Radhakrishnan *et al.* 1980).

A structurally based constitutive formulation for ischaemic and necrotic myocardium will need to account for structural and mechanical data. Substantial changes in myocardial cell and matrix structure can occur within 20 min of acute ischaemia. *Ex vivo* uniaxial (Przyklenk *et al.* 1987) and biaxial (Gupta *et al.* 1994) tests suggest that infarct stiffness does not change significantly in the first hours to days after infarction. However, changes in residual stress can occur within 30 min of coronary occlusion (Summerour *et al.* 1998), and may be related to oedema. Based on the finding that a variety of anti-inflammatory agents increase infarct expansion (Jugdutt 1985), swelling has been proposed as a determinant of stiffness during the necrotic phase of healing but has been explicitly incorporated in few constitutive models (Bogen 1987).

(*a*) *Myocardial scar tissue*

Myocardial scar tissue impairs ventricular pump function by decreasing the amount of contracting myocardium contributing to ejection, by stretching during systole and reducing forward stroke volume, and by interfering with shortening and thickening of the adjacent myocardium. Published reports have concluded that depression of left ventricular function during post-infarction healing depends not only on scar size (Choong *et al.* 1989) but also on scar stiffness (Bogen *et al.* 1984).

Early pressure-segment length measurements (Theroux *et al.* 1977) and *ex-vivo* uniaxial studies (Connelly *et al.* 1992; Przyklenk *et al.* 1987) provided one-dimensional data about the evolution of infarct properties over time, but *ex-vivo* biaxial (Gupta *et al.* 1994) and *in-vivo* studies (Holmes *et al.* 1994, 1997; Lima *et al.* 1995) showed that the mechanics of myocardial scar are inherently three dimensional. Although collagen content in healing ovine myocardial scar tissue increased steadily during the first six weeks after infarction, longitudinal stress at 15% equibiaxial extension peaked one week after infarction and circumferential stress two weeks after infarction (Gupta *et al.* 1994). This anisotropy of myocardial scar is central to its impact on ventricular function. We found that highly anisotropic porcine myocardial scar resists stretching in the circumferential direction while deforming compatibly with adjacent myocardium in the longitudinal and radial directions and proposed that scar anisotropy thereby preserves systolic function in the infarcted ventricle (Holmes *et al.* 1997).

A natural starting point for modelling the mechanics of myocardial scar tissue is the structure of large collagen fibres in the scar. Large collagen fibres in both canine

(Whittaker *et al.* 1989) and porcine (Holmes & Covell 1996) myocardial scars are highly aligned in each transmural layer; mean collagen fibre angle varies transmurally with a pattern similar to normal muscle fibres but spanning a smaller range of angles through the wall. Given the high area fraction occupied by these large fibres and their expected axial stiffness, we assumed that scar material properties arise primarily from the tensile stiffness of large collagen fibres. We represented myocardial scar as an incompressible hyperelastic material with an exponential strain-energy function containing an isotropic term and a family of terms related to axial deformation of collagen fibres:

$$W = \tfrac{1}{2}C_1(\mathrm{e}^Q - 1), \qquad Q = C_2(I_1 - 3) + C_3(\text{fibre strain terms}). \tag{4.1}$$

At each transmural depth, we expressed the orientation of individual fibres relative to the local mean fibre angle and the axial strain of each fibre in terms of strain components in an axis system aligned with the mean fibre, mean cross-fibre, and radial directions. Since the large collagen fibres are oriented in planes perpendicular to the radius, the radial component of all fibre vectors was neglected:

$$\alpha_i = \theta_i - \theta_{\mathrm{mean}}, \qquad E_\alpha = \boldsymbol{n}_\alpha \boldsymbol{E} \boldsymbol{n}_\alpha = \begin{bmatrix} \cos\alpha \\ \sin\alpha \\ 0 \end{bmatrix}^{\mathrm{T}} \begin{bmatrix} E_{\mathrm{ff}} & E_{\mathrm{fc}} & E_{\mathrm{fr}} \\ E_{\mathrm{cf}} & E_{\mathrm{cc}} & E_{\mathrm{cr}} \\ E_{\mathrm{rf}} & E_{\mathrm{rc}} & E_{\mathrm{rr}} \end{bmatrix} \begin{bmatrix} \cos\alpha \\ \sin\alpha \\ 0 \end{bmatrix} \tag{4.2}$$

Summing over a discrete distribution of k individually measured fibre angles weighted by histological collagen area fraction measured at each depth, yielded a strain-energy function with eight material constants, five of which were readily determined from the measured large collagen fibre distribution within the scar. The remaining three constants scale the steepness of the exponential (C_1) and the relative contributions of the large collagen fibres (C_2) to the isotropic background (C_3):

$$\left.\begin{aligned} W &= \tfrac{1}{2}C_1(\mathrm{e}^Q - 1), \\ Q = C_2(I_1 - 3) + C_3(&C_4E_{\mathrm{ff}}^2 + C_5E_{\mathrm{cc}}^2 + C_6(2E_{\mathrm{ff}}E_{\mathrm{cc}} + E_{\mathrm{fc}}^2 + 2E_{\mathrm{fc}}E_{\mathrm{cf}} + E_{\mathrm{cf}}^2) \\ &+ C_7(2E_{\mathrm{ff}}E_{\mathrm{fc}} + 2E_{\mathrm{ff}}E_{\mathrm{cf}}) + C_8(2E_{\mathrm{fc}}E_{\mathrm{cc}} + 2E_{\mathrm{cf}}E_{\mathrm{cc}})), \end{aligned}\right\} \tag{4.3}$$

where

$$\left.\begin{aligned} C_4 &= \sum_1^k h(\alpha_j)(\cos\alpha_j)^4, & C_5 &= \sum_1^k h(\alpha_j)(\sin\alpha_j)^4, \\ C_6 &= \sum_1^k h(\alpha_j)(\sin\alpha_j)^2(\cos\alpha_j)^2, & C_7 &= \sum_1^k h(\alpha_j)(\sin\alpha_j)(\cos\alpha_j)^3, \\ C_8 &= \sum_1^k h(\alpha_j)(\sin\alpha_j)^3(\cos\alpha_j), & h(\alpha) &= \frac{\text{area fraction}}{k}, \\ & & \alpha &= \alpha_j, \quad j = 1, 2, \ldots, k. \end{aligned}\right\} \tag{4.3 \textit{cont.}}$$

Values for constants C_4 through C_8 calculated from measured collagen fibre angle distributions in three-week transmural porcine scar are shown in table 2. Transmural variation in the angular dispersion of large collagen fibres about the local mean resulted in large transmural differences in anisotropy as reflected in the ratio C_4/C_5.

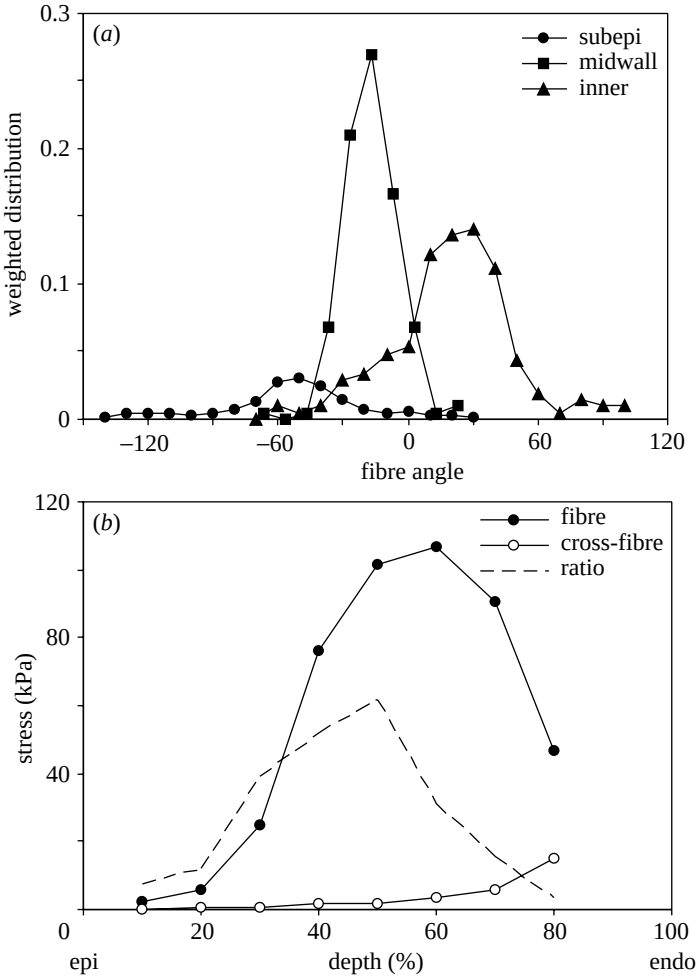

Figure 4. Transmural variations in scar anisotropy predicted from collagen fibre structure. (*a*) Measured normalized fibre distributions weighted by collagen area fraction at each depth; fibres are both more closely aligned and more dense in the midwall than in other layers. (*b*) Predicted anisotropy in simulated 15% equibiaxial extension varies strongly across the wall ('ratio' is the ratio of fibre stress to cross-fibre stress, plotted on the same scale).

The predicted ratio of stress in the mean fibre and cross-fibre directions at 15% equibiaxial extension in a typical simulation ($C_1 = 0.5$ kPa, $C_2 = 1.0$, $C_3 = 100$) varied from 3 in the subendocardium to 62 in the midwall (figure 4). Simulated tests of full-thickness specimens using these constants agreed reasonably well with equibiaxial test data (Gupta *et al.* 1994).

5. Summary

The constitutive properties of myocardium are three dimensional, anisotropic, nonlinear and time dependent. Formulating useful constitutive laws requires a combination of multi-axial tissue testing *in vitro*, microstructural modelling based on quantitative morphology, statistical parameter estimation, and validation and opti-

Table 2. *Material constants calculated from measured large collagen fibre angle distributions in a three-week old porcine myocardial scar*

% depth	C_4	C_5	C_6	C_7	C_8
10	0.1140	0.0213	0.0133	0.0001	−0.0001
20	0.2211	0.0161	0.0224	0.0056	−0.0014
30	0.4816	0.0065	0.0260	0.0014	−0.0014
40	0.7458	0.0058	0.0287	0.0000	0.0000
50	0.8215	0.0042	0.0292	0.0021	−0.0021
60	0.8235	0.0101	0.0367	−0.0055	0.0055
70	0.7615	0.0256	0.0454	0.0038	−0.0038
80	0.4971	0.1006	0.1006	0.1146	0.0527

mization using data from intact heart preparations. Recent models capture some important properties of healthy and diseased myocardium including: the nonlinear interactions between the responses to different loading patterns; the influence of the laminar myofibre sheet architecture; the effects of transverse stresses developed by the myocytes; and the relationship between collagen fibre architecture and mechanical properties in healing scar tissue after myocardial infarction.

References

Bogen, D. K. 1987 Strain energy descriptions of biological swelling. II. Multiple fluid compartment models. *ASME J. Biomech. Engng* **109**, 257–262.

Bogen, D. K., Rabinowitz, S. A., Needleman, A., McMahon, T. A. & Abelmann, W. H. 1980 An analysis of the mechanical disadvantage of myocardial infarction in the canine left ventricle. *Circ. Res.* **47**, 728–741.

Bogen, D. K., Needleman, A. & McMahon, T. A. 1984 An analysis of myocardial infarction: the effect of regional changes in contractility. *Circ. Res.* **55**, 805–815.

Bovendeerd, P. H. M., Huyghe, J. M., Arts, T., van Campen, D. H. & Reneman, R. S. 1994 Influence of endocardial–epicardial crossover of muscle fibres on left ventricular wall mechanics. *J. Biomech.* **27**, 941–951.

Choong, C. Y., Gibbons, E. F., Hogan, R. D., Franklin, T. D., Nolting M., Mann, D. L. & Weyman, A. E. 1989 Relationship of functional recovery to scar contraction after myocardial infarction in the canine left ventricle. *Am. Heart J.* **117**, 819–829.

Connelly, C. M., Ngoy S., Schoen, F. J. & Apstein, C. S. 1992 Biomechanical properties of reperfused transmural myocardial infarcts in rabbits during the first week after infarction: implications for left ventricular rupture. *Circ. Res.* **71**, 401–413.

Costa, K. D., May-Newman, K. D., Farr D., O'Dell, W. G., McCulloch, A. D. & Omens, J. H. 1997 Three-dimensional residual strain in midanterior canine left ventricle. *Am. J. Physiol.* **273**, H1968–H1976.

Costa, K. D., Takayama, Y., McCulloch, A. D. & Covell, J. W. 1999 Laminar fiber architecture and three-dimensional systolic mechanics in canine ventricular myocardium. *Am. J. Physiol.* **276**, H595–H607.

Criscione, J. C., Douglas, A. S. & Hunter, W. C. 2001 Physically based strain invariant set for materials exhibiting transversely isotropic behavior. *J. Mech. Phys. Solids* **49**, 871–897.

Demer, L. L. & Yin, F. C. P. 1983 Passive biaxial mechanical properties of isolated canine myocardium. *J. Physiol. Lond.* **339**, 615–630.

Emery, J. L. & Omens, J. H. 1997 Mechanical regulation of myocardial growth during volume-overload hypertrophy in the rat. *Am. J. Physiol.* **273**, H1198–H1204.

Emery, J., Omens, J. & McCulloch, A. 1997 Biaxial mechanics of the passively overstretched left ventricle. *Am. J. Physiol. Heart Circ. Physiol.* **272**, H2299–H2305.

Emery, J., Omens, J., Mathieu-Costello, O. & McCulloch, A. 1998 Structural mechanisms of acute ventricular strain softening. *J. Cardiovasc. Med. Sci.* **1**, 241–250.

Feneis, H. 1943 Das Gefüge des Herzmuskels bei Systole und Diastole. *Morph. Jahrb.* **89**, 371–406.

Granzier, H. L. & Irving, T. C. 1995 Passive tension in cardiac muscle: contribution of collagen, titin, microtubules, and intermediate filaments. *Biophys. J.* **68**, 1027–1044.

Guccione, J. M. & McCulloch, A. D. 1991 Finite element modelling of ventricular mechanics. In *Theory of heart: biomechanics, biophysics and nonlinear dynamics of cardiac function* (ed. L. Glass, P. J. Hunter & A. D. McCulloch), pp. 121–144. Springer.

Guccione, J. M., McCulloch, A. D. & Waldman, L. K. 1991 Passive material properties of intact ventricular myocardium determined from a cylindrical model. *ASME J. Biomech. Engng* **113**, 42–55.

Guccione, J. M., Waldman, L. K. & McCulloch, A. D. 1993 Mechanics of active contraction in cardiac muscle. Part II. Cylindrical models of the systolic left ventricle. *ASME J. Biomech. Engng* **115**, 82–90.

Guccione, J. M., Costa, K. D. & McCulloch, A. D. 1995 Finite element stress analysis of left ventricular mechanics in the beating dog heart. *J. Biomech.* **28**, 1167–1177.

Gupta, K. B., Ratcliffe, M. B., Fallert, M. A., Edmunds Jr, L. H. & Bogen, D. K. 1994 Changes in passive mechanical stiffness of myocardial tissue with aneurysm formation. *Circulation* **89**, 2315–2326.

Halperin, H. R., Chew, P. H., Weisfeldt, M. L., Sagawa K., Humphrey, J. D. & Yin, F. C. P. 1987 Transverse stiffness: a method for estimation of myocardial wall stress. *Circ. Res.* **61**, 695–703.

Holmes, J. W. & Covell, J. W. 1996 Collagen fiber orientation in myocardial scar tissue. *Cardiovasc. Pathobiol.* **1**, 15–22.

Holmes, J. W., Yamashita, H., Waldman, L. K. & Covell, J. W. 1994 Scar remodeling and transmural deformation after infarction in the pig. *Circulation* **90**, 411–420.

Holmes, J. W., Nunez, J. A. & Covell, J. W. 1997 Functional implications of myocardial scar structure. *Am. J. Physiol.* **272**, H2123–H2130.

Humphrey, J. D., Strumpf, R. K. & Yin, F. C. P. 1990*a* Determination of a constitutive relation for passive myocardium. I. A new functional form. *J. Biomech. Engng* **112**, 333–339.

Humphrey, J. D., Strumpf, R. K. & Yin, F. C. P. 1990*b* Determination of a constitutive relation for passive myocardium. II. Parameter estimation. *J. Biomech. Engng* **112**, 340–346.

Humphrey, J. D., Strumpf, R. K. & Yin, F. C. P. 1990*c* Biaxial mechanical behavior of excised ventricular epicardium. *Am. J. Physiol.* **259**, H101–H108.

Huyghe, J. M., Arts, T., van Campen, D. H. & Reneman, R. S. 1992 Porous medium finite element model of the beating left ventricle. *Am. J. Physiol.* **262**, H1256–H1267.

Iimoto, D., Covell, J. & Harper, E. 1988 Increase in crosslinking of type I and type III collagens associated with volume overload hypertrophy. *Circ. Res.* **63**, 399–408.

Janz, R. F. & Waldron, R. J. 1977 Predicted effect of chronic apical aneurysms on the passive stiffness of the human left ventricle. *Circ. Res.* **42**, 255–263.

Johnson, B. & Hoger, A. 1995 Formulation of constitutive equations for residually stressed materials by use of a virtual configuration. *J. Elasticity* **41**, 177–215.

Jugdutt, B. I. 1985 Delayed effects of early infarct-limiting therapies on healing after myocardial infarction. *Circulation* **72**, 907–914.

Kang, T. & Yin, F. C. P. 1996 The need to account for residual strains and composite nature of heart wall in mechanical analyses. *Am. J. Physiol.* **271**, H947–H961.

Karlon, W., Covell, J., McCulloch, A. & Omens, J. 1998 Relationship between myofiber disarray and epicardial shortening in hypertrophic cardiomyopathy (abstract). *Circulation Suppl.* **98**, I761.

Landesberg, A., Beyar, R. & Sideman, S. 1995 Crossbridge dynamics in muscle contraction. *Adv. Exp. Med. Biol.* **382**, 137–153.

LeGrice, I. J., Smaill, B. H., Chai, L. Z., Edgar, S. G., Gavin, J. B. & Hunter, P. J. 1995*a* Laminar structure of the heart: ventricular myocyte arrangement and connective tissue architecture in the dog. *Am. J. Physiol.* **269**, H571–H582.

LeGrice, I. J., Takayama, Y. & Covell, J. W. 1995*b* Transverse shear along myocardial cleavage planes provides a mechanism for normal systolic wall thickening. *Circ. Res.* **77**, 182–193.

LeGrice, I., Hunter, P., Young, A. & Smail, B. 2001 The architecture of the heart: a data-based model. *Phil. Trans. R. Soc. Lond.* A **359**, 1217–1232.

Lima, J. A., Ferrari, V. A., Reichek, N., Kramer, C. M., Palmon, L., Llaneras, M. R., Tallant, B., Young, A. A. & Axel, L. 1995 Segmental motion and deformation of transmurally infarcted myocardium in acute postinfarct period. *Am. J. Physiol. Heart Circ. Physiol.* **268**, H1304–H1312.

Lin, D. H. & Yin, F. C. 1998 A multiaxial constitutive law for mammalian left ventricular myocardium in steady-state barium contracture or tetanus. *J. Biomech. Engng* **120**, 504–517.

MacKenna, D. A., Vaplon, S. M. & McCulloch, A. D. 1997 Microstructural model of perimysial collagen fibers for resting myocardial mechanics during ventricular filling. *Am. J. Physiol.* **273**, H1576–H1586.

Mazhari, R., Omens, J., Covell, J. & McCulloch, A. 2000 Structural basis of regional dysfunction in acutely ischemic myocardium. *Cardiovasc. Res.* **47**, 284–293.

Michailova, A. & Spassov, V. 1997 Computer simulation of excitation–contraction coupling in cardiac muscle: a study of the regulatory role of calcium binding to troponin C. *Gen. Physiol. Biophys.* **16**, 29–38.

Nash, M. & Hunter, P. 2001 Computational mechanics of the heart. *J. Elasticity.* (In the press.)

Novak, V. P., Yin, F. C. P. & Humphrey, J. D. 1994 Regional mechanical properties of passive myocardium. *J. Biomech.* **27**, 403–412.

Omens, J. H. & Fung, Y. C. 1990 Residual strain in rat left ventricle. *Circ. Res.* **66**, 37–45.

Omens, J. H., May, K. D. & McCulloch, A. D. 1991 Transmural distribution of three-dimensional strain in the isolated arrested canine left ventricle. *Am. J. Physiol.* **261**, H918–H928.

Omens, J. H., MacKenna, D. A. & McCulloch, A. D. 1993 Measurement of strain and analysis of stress in resting rat left ventricular myocardium. *J. Biomech.* **26**, 665–676.

Przyklenk, K., Connelly, C. M., McLaughlin, R. J., Kloner, R. A. & Apstein, C. S. 1987 Effect of myocyte necrosis on strength, strain, and stiffness of isolated myocardial strips. *Am. Heart J.* **114**, 1349–1359.

Rademakers, F. E., Rogers, W. J., Guier, W. H., Hutchins, G. M., Siu, C. O., Weisfeldt, M. L., Weiss, J. L. & Shapiro, E. P. 1994 Relation of regional cross-fiber shortening to wall thickening in the intact heart: three-dimensional strain analysis by NMR tagging. *Circulation* **89**, 1174–1182.

Radhakrishnan, S., Ghista, D. & Jayaraman, G. 1980 Mechanical analysis of the development of left ventricular aneurysms. *J. Biomech.* **13**, 1031–1039.

Rice, J., Winslow, R. & Hunter, W. 1999 Comparison of putative cooperative mechanisms in cardiac muscle: length dependence and dynamic responses. *Am. J. Physiol. Heart Circ. Physiol.* **276**, H1734–H1754.

Rijcken, J., Bovendeerd, P. H., Schoofs, A. J., van Campen, D. H. & Arts, T. 1999 Optimization of cardiac fiber orientation for homogeneous fiber strain during ejection. *Ann. Biomed. Engng* **27**, 289–297.

Rodriguez, E. K., Omens, J. H., Waldman, L. K. & McCulloch, A. D. 1993 Effect of residual stress on transmural sarcomere length distribution in rat left ventricle. *Am. J. Physiol.* **264**, H1048–H1056.

Rodriguez, E. K., Hoger, A. & McCulloch, A. D. 1994 Stress-dependent finite growth law in soft elastic tissues. *J. Biomech.* **27**, 455–467.

Sacks, M. 1999 A method for planar biaxial mechanical testing that includes in-plane shear. *J. Biomech. Engng* **121**, 551–555.

Sacks, M. S. & Chuong, C. J. 1993 Biaxial mechanical properties of passive right ventricular free wall myocardium. *ASME J. Biomech. Engng* **115**, 202–205.

Schoenberg, M. 1980*a* Geometrical factors influencing muscle force development. I. The effect of filament spacing upon axial forces. *Biophys. J.* **30**, 51–67.

Schoenberg, M. 1980*b* Geometrical factors influencing muscle force development. II. Radial forces. *Biophys. J.* **30**, 69–77.

Spotnitz, H. M., Spotnitz, W. D., Cottrell, T. S., Spiro, D. & Sonnenblick, E. H. 1974 Cellular basis for volume related wall thickness changes in the rat left ventricle. *J. Molec. Cell Cardiol.* **6**, 317–331.

Summerour, S., Emery, J., Fazeli, B., Omens, J. & McCulloch, A. 1998 Residual strain in ischemic ventricular myocardium. *J. Biomech. Engng* **120**, 710–714.

ter Keurs, H. 1995 Sarcomere function and crossbridge cycling. *Adv. Exp. Med. Biol.* **382**, 125–135.

Theroux, P., Ross Jr, J., Franklin, D., Covell, J. W., Bloor, C. M. & Sasayama, S. 1977 Regional myocardial function and dimensions early and late after myocardial infarction in the unanesthetized dog. *Circ. Res.* **40**, 158–165.

Usyk, T. P., Mazhari, R. & McCulloch, A. D. 2001 Effect of laminar orthotropic myofiber architecture on regional stress and strain in the canine left ventricle. *J. Elasticity.* (In the press.)

Vetter, F. J. & McCulloch, A. D. 2000 Three-dimensional stress and strain in passive rabbit left ventricle: a model study. *Ann. Biomed. Engng* **28**, 781–792.

Waldman, L. K., Nossan, D., Villarreal, F. & Covell, J. W. 1988 Relation between transmural deformation and local myofiber direction in canine left ventricle. *Circ. Res.* **63**, 550–562.

Weis, S. M., Emery, J. L., Becker, K. D., McBride Jr, D. J., Omens, J. H. & McCulloch, A. D. 2000 Myocardial mechanics and collagen structure in the osteogenesis imperfecta murine (*oim*). *Circ. Res.* **87**, 663–669.

Whittaker, P., Boughner, D. R. & Kloner, R. A. 1989 Analysis of healing after myocardial infarction using polarized light microscopy. *Am. J. Pathol.* **134**, 879–893.

Yin, F. C. P., Strumpf, R. K., Chew, P. H. & Zeger, S. L. 1987 Quantification of the mechanical properties of noncontracting canine myocardium under simultaneous biaxial loading. *J. Biomech.* **20**, 577–589.

Zahalak, G. I. 1996 Non-axial muscle stress and stiffness. *J. Theor. Biol.* **182**, 59–84.

Zahalak, G. I., de Laborderie, V. & Guccione, J. M. 1999 The effects of cross-fiber deformation on axial fiber stress in myocardium. *J. Biomech. Engng* **121**, 376–385.